Effects of plant roots on soil-water retention and induced suction in vegetated soil

A. K. Leung, A. Garg, and C. W. W. Ng

Name: Dr Anthony Kwan, LEUNG* (Corresponding author)

Title: Lecturer

Affiliation: Division of Civil Engineering, University of Dundee

Address: Division of Civil Engineering, University of Dundee, Nethergate, Scotland, UK, DD1 4HN

E-mail: a.leung@dundee.ac.uk, **Telephone**: +44(0)1382 384390, **Fax**: +44(0)1382 384389

Name: Dr Ankit, GARG

Title: Visiting research scholar

Affiliation: Department of Civil and Environmental Engineering, Hong Kong University of Science and Technology

Address: Department of Civil and Environmental Engineering, Hong Kong University of Science and Technology, Clear Water Bay, Kowloon, Hong Kong

Name: Dr Charles Wang Wai, NG

Title: Chair Professor in Civil and Environmental Engineering

Affiliation: Department of Civil and Environmental Engineering, Hong Kong University of Science and Technology

Address: Department of Civil and Environmental Engineering, Hong Kong University of Science and Technology, Clear Water Bay, Kowloon, Hong Kong

Abstract:

Plant evapotranspiration (ET) is considered to be a hydrological effect that would induce soil suction and hence influence the stability of geotechnical infrastructure. However, other hydrological effect, such as the change of soil water retention curve (SWRC) induced by roots, is generally ignored. This study aims to investigate and compare the effects of root-induced changes in SWRC with the effects of ET on suction responses in clayey sand. Two series of laboratory tests together with 21 numerical transient seepage analyses were conducted. A tree species, *Schefflera heptaphylla*, which is commonly used for ecological restoration in many subtropical regions, was selected for investigation. In order to consider any effects of tree variability on induced suction, six tree individuals with similar age were tested with and without the supply of light. It is revealed that under dark condition when ET was minimal, vegetated soil could induce higher suction than bare soil by 100% after subjecting to a wetting event with a return period of 100 years. This may be explained by the increases in the air-entry value and the size of hysteresis loop induced by roots. Water balance calculation from the numerical analyses shows that even under the supply of light, the amount of ET was only 1.7% of the total volume of water infiltrated. This means that during the wetting event, the contribution of ET and root-water uptake to induced suction in vegetated soil was relatively little, as compared with the effects of root-induced change in SWRC.

1.   Introduction

The use of plant roots has been generally recognised as an environmentally and ecologically friendly engineering solution that can improve the stability of man-made geotechnical infrastructure such as compacted slopes/embankments and landfill covers. It is well-known that upon evapotranspiration (ET), soil moisture would be reduced through root-water uptake, and this would consequently induce suction in the soil (Biddle, 1983; Blight, 2003; Hemmati et al., 2012). Changes of ET-induced suction have significant impact on the performance of the infrastructure because this would result in the changes of soil shear strength (Gan et al., 1988) and hydraulic conductivity (Ng and Leung, 2012). They are the two vital soil properties that govern the transient seepage and stability of geotechnical infrastructure.

In addition to plant ET, another hydrological effect of plant roots that could potentially affect the soil suction is the change of soil water retention behaviour induced by roots. Limited studies showed that roots could change soil structures, through mainly (i) volumetric occupancy of roots in soil pore space (Scanlan and Hinz, 2010; Scholl et al., 2014); (ii) water retention in roots (Taleisnik et al., 1999); (iii) the release of root exudates (Grayston, 1997; Traoré et al., 2000). It is well-recognised that soil water retention curve (SWRC) primarily depends on soil pore size and its distribution (Romero et al., 1999; Ng and Pang, 2000; Ng and Leung, 2012). It is thus anticipated that the changes in soil structures due to the above processes would induce some changes in pore-size distribution, and consequently SWRC. However, rare experimental study is available to report

any root-induced change in SWRC, and its effects on suction response.

Extensive studies have reported the responses of suction in soil induced by plants (Lim et al., 1996; Simon and Collison, 2002; Smerthurst et al., 2006; Leung and Ng, 2013, 2014; Ng et al., 2013, 2014; Rahardjo et al., 2014; Leung, 2014). However, it is difficult, if not impossible, to isolate the effects of root-induced change in SWRC, and also to identify to what extent this would affect suction response, as compared to the effects of plant ET. When assessing slope stability, it is vital to determine the minimum suction that could be induced during wetting in night time, rather than the maximum suction induced during drying in day time. This is because at night there is no supply of solar radiation, and any suction induced by plant ET and the associated root-water uptake would be minimal. In this case, the effects of plant roots on suction responses could be mainly affected by any modification of SWRC. It is thus important to quantify any root-induced SWRC change, and hence the suction responses, so as to carry out more reliable water balance and stability calculations for a slope.

The objectives of this study are to (i) explore and compare the effects of the two hydrological mechanisms, namely (a) change of soil water retention ability induced by roots (denoted as M1) and (b) plant ET and the associated root-water uptake (denoted as M2), on suction induced in vegetated soil, and then (ii) to identify and quantify their relative importance/contribution. Two series of laboratory tests were conducted in an atmosphere-controlled room. The measured results were then subsequently interpreted through 21 numerical simulation of transient seepage in

unsaturated, vegetated soil.

2. Experimental test programme

2.1 *Test plan*

Two series of laboratory tests were carried out. The objective of the first series was to investigate the contribution of solely mechanism M1 to the suction response in vegetated soil. In this series, both bare soil and vegetated soil were subjected to an identical wetting-drying cycle under dark condition in an atmosphere-controlled plant room. Under the dark condition, mechanism M2 was eliminated since no energy was available for energy interception, and transpiration. This would thus quantify the effects of plant roots on minimum suction induced during a wetting event when ET cannot take place, for instances, at night time (i.e., when no solar radiation is supplied). The second series of tests was the repetition of the first series, but with the supply of light. In this case, effects of either or both mechanisms M1 and M2 would contribute to any suction change.

To assist the interpretation of test results through water balance calculation, soil water retention curves (SWRCs) of both bare and vegetated soil were measured after the two series of tests. This intends to provide evidence to support mechanism M1 and hence to help explain any difference of suction responses observed from the first series of tests. In addition, the biomass of shoot and root of all six tree individuals were also measured. These properties are useful to help understand any contribution of root-water uptake (mechanism M2) to suction response in vegetated soil in the second series of test.

2.2   *Experimental setup and instrumentation*

In this study, eight plastic test boxes (two bare and six vegetated) were designed. Fig. 1 shows the overview of the test setup of a typical vegetated box. The cross-section area and the depth of each test box are 300 x 300 mm^2 and 300 mm, respectively. Soil with a thickness of 280 mm was compacted in each box, while a tree individual was transplanted at the centre of each vegetated box. The dimension of each box is sufficiently large to test a tree individual, which has an average root depth of 103.5 mm and lateral spread of 80 mm. At the bottom of each box, there are nine drainage holes with a diameter of 5 mm each for bottom drainage during testing. All eight boxes were tested in a plant room, where the atmospheric conditions including air temperature, radiant energy and relative humidity (RH) of air were maintained constant at 22.3±1 ºC, 15.3±1 MJ m^{-2} d^{-1} and 53±7%, respectively. Potential evaporation (PE) in bare soil may be determined by Penman equation (Penman, 1948), which is derived based on the energy balance at the soil-atmosphere interface, where mass transfer is taken into account through Dalton's law. This equation estimates the potential amount of liquid water being escaped from a soil surface as vapour water (i.e., known as potential evaporation, PE), depending on the atmospheric condition. Penman equation may be expressed by Eq (1) as follows:

$$PE = \frac{\frac{\Delta R_n}{\lambda} + \gamma E_a}{\Delta + \gamma} , \qquad \text{where } E_a = 0.165 \times (e_s - e_a)\left(0.8 + \frac{u}{100}\right) \qquad (1)$$

where Δ is slope of vapour pressure curve (kPa ºC^{-1}); R_n is radiant energy (MJ m^{-2} d^{-1}), λ is latent heat of vaporisation (MJ kg^{-1}); γ is psychometric constant (kPa ºC^{-1}); e_s is saturated vapour pressure

(kPa); e_a is actual vapour pressure (kPa); ($e_s − e_a$) is vapour pressure deficit (kPa); u is wind speed

(m s^{-1}). For the given controlled atmospheric condition in the plant room and the parameters adopted

in Table 1, the rate of PE estimated by Eq (1) is 5.04 mm d^{-1}. On the other hand, potential

evapotranspiration (PET) in vegetated soil can be determined by Penman-Monteith equation (Allen

et al., 1998). This equation modifies Penman equation by introducing resistance factors, namely

crop canopy resistance, r_c (s m^{-1}) and aerodynamic resistance, r_a (s m^{-1}). r_c describes the resistance

of vapour flow through stomata openings and leaf surface, and is typically correlated with Leaf Area

Index (LAI; a dimensionless index defining the ratio of total one-sided green leaf area to projected

area of an individual plant on soil surface in plan). r_a describes friction from air flowing over leaf

surfaces and is therefore a function of wind speed. Penman-Monteith equation may be expressed in

Eq. (2) as follows:

$$\text{PET} = \left[\frac{\Delta(R_n − G_s)}{\Delta + \gamma\left(1 + \frac{r_c}{r_a}\right)} + \frac{\rho c_p (e_s − e_a)/r_a}{\Delta + \gamma\left(1 + \frac{r_c}{r_a}\right)} \right] \tag{2}$$

where G_s is soil heat flux density (J m^{-2} d^{-1}) (assumed negligible as the amount is minimal as

compared to R_n; Allen et al., 1998); ρ is air density (kg m^{-3}); and c_p is specific heat of moist air (kJ

kg^{-1} °C^{-1}). Depending on tree LAI and using the parameters shown in Table 1, the rate of PET ranges

from 2.51 − 3.37 mm d^{-1}. It should not be surprised that the estimated range of PET is lower than PE

as more energy was needed to overcome both r_c and r_a at the leave-atmosphere interface (Allen et al.,

1998).

Negative pore-water pressure (PWP) induced in each test box was measured by miniature

tensiometers (Model 2100F; Soilmoisture Equipment Corp). Each one has a ceramic cup (i.e., the sensing element) of 6 mm in diameter and it is 25 mm long. Laboratory calibration shows that the accuracy of each tensiometer is ±1 kPa, while the response time is faster than 5 min. A vertical array of four tensiometers (denoted T1, T2, T3 and T4 in Fig. 1) was installed along the centreline of each test box at 30, 80, 140 and 210 mm depths. Each tensiometer, which was fully saturated with deaired water, is capable of measuring suction from 0 to 80 kPa. Since the bottom of each box was allowed for free drainage throughout the entire test, it is thus reasonable to assume pore-air pressure to be atmospheric. Hence, any negative PWP measured by each tensiometer is equal to suction. In addition, a quantum sensor was used to measure radiant energy received on the surface of bare and vegetated soil. Each quantum sensor was placed at the centre of the soil surface, where the leaf area projected on plan is the largest. The measurement would thus reflect the maximum ability of each tree individual to intercept radiant energy for transpiration and inducing suction. Since the purpose of measuring energy interception is to interpret any tree-induced suction during a wetting event, it is useful to determine the greatest energy interception, rather than other lower values obtained from other positions of the box, where the projected leaf area is lower. It should be pointed out that spatial variation of radiant energy is not the focus of this study. Each quantum sensor measures photosynthetic photon flux density (μmol m^{-2} s^{-1}), which is then converted to radiant energy (MJ m^{-2} d^{-1}) using Planck relation, given the known waveband of the light (400 to 700 nm in this case) applied in the plant room. Any difference between the applied and measured radiant energy is equal

to the energy intercepted by tree leaves, neglecting (1) reflected radiant energy at each individual

leaf surface due to low albedo (Taha et al., 1988); (2) radiant energy used to heat up air due to low

air density; and (3) energy intercepted by tree stem and branches because of their relatively small

total surface area as compared to that of leaves.

2.3   *Soil type and preparation method*

The soil type selected for investigation is completely decomposed granite (CDG), which is

commonly found in Hong Kong. The gravel, sand, silt and clay contents of CDG were determined to

be 19%, 42%, 27% and 12%, respectively. The coefficients of uniformity and curvature are found to

be 13.3 and 1.6 respectively, and this CDG is thus classified as a well-graded soil. The plastic limit

and liquid limit of the silt and clay fraction of the CDG were found to be 26% and 44%, respectively.

Based on the measured particle-size distribution and Atterberg limit, CDG is thus classified as

clayey sand with gravel (SC), according to the Unified Soil Classification System (USCS). The

volumetric field capacity, which refers to an equilibrium moisture content held in soil (by volume)

after excess water is drained away by gravity (Veihmeyer and Hendrickson, 1931), is found to be

16% − 19%. It should be noted that volumetric field capacity is different from saturated volumetric

water content, as the former term suggests that the soil pore space is not completely filled with water

but this is the case for the latter term. Volumetric field capacity of soil has been identified to be an

ideal soil moisture level that promotes plant transpiration, root growth and its establishment with the

surrounding soil during the early stage of transplantation (Wang et al., 2006). This would prevent

plants from developing significant oxygen stress (i.e., lack of soil aeration; Dasberg and Bakker, 1970), which could severely suppress plant metabolism and transpiration. In all eight test boxes, under-compaction method (Ladd, 1978) was adopted to compact CDG at a targeted dry density of 1496 kg m^{-3} (i.e., equivalent to relative compaction, RC, of 80%) and water content of 13% by mass. The bare boxes tested under light and dark condition are denoted as B_L and B_D, respectively.

2.4 *Selected tree species and growth condition*

The vegetation type selected for investigation is a tree species, *Schefflera heptaphylla* (also known as Ivy tree). This species is selected because of (i) the recognition of its significant ornamental and ecological values for slope rehabilitation and reforestation (GEO, 2011); (ii) their ability of drought tolerant at warm climates of the world (Carrow et al., 1996; Hau and Corlett, 2003; Hu et al., 2010); and (iii) their commonness in many parts of the South-East Asia including Hong Kong, India and Malaysia (Hau and Corlett, 2003; Frodin et al., 2010). Note that *S. heptaphylla* is not a crop species, and thus it does not need to be grown in soil that has rich organic contents and nutrient concentration (Vetterlein et al., 1993; Roberts, 2000). *S. heptaphylla* also does not require frequent irrigation and harvesting (Carrow et al., 1996; Hau and Corlett, 2003), which are usually important for crop species when crop yield is of concern (Zhang et al., 2004).

In this study, six tree individuals, which were previously grown in CDG (i.e., the same soil type tested in this study) in a nursery, were transplanted to six separate test boxes. Each vegetated box was irrigated every two days over two months. This aims to maintain the level of average soil

moisture close to the field capacity of the soil. The duration of two months of frequent irrigation schedule has been shown to be sufficient for plant roots to establish with the surrounding soil (Wang et al., 2006). Note that fertiliser was purposely not added to all vegetated soil. This aims to prevent any osmotic suction induced due to solute concentrations in pore water (Krahn and Fredlund, 1972).

Due to the variability of tree species, the six tree individuals have different properties. They have a mean shoot height of 425 mm with a standard deviation of 12 mm, and have a mean LAI of 2.62 with a standard deviation of 1.07. Three of these six vegetated test boxes were used for the first test series, and they are denoted as T1_D, T2_D and T3_D. The remaining three boxes that were used in the second series are denoted as T1_L, T2_L and T3_L. Table 2 summarises some properties of the six individuals.

2.5 *Test procedures*

For the first series of test conducted under dark condition (i.e., bare box B_D and the three vegetated boxes T1_D, T2_D and T3_D), all boxes were subjected to a two-stage test. Prior to testing, it was intended to establish similar initial suction distributions among all four boxes. Soil surface of each box was ponded until (i) suctions at all four instrument depths decreased to 0 kPa and (ii) percolation through the nine drainage holes at the box base was observed. Then, all four boxes were exposed under the identical atmospheric conditions in the plant room. The nine bottom holes of each box remained open for free drainage, preventing from any air entrapment and its effect on suction responses during a wetting event (Wang et al., 1997, 1998). Variations of suction were monitored

continuously. When their suction profiles were found to be similar, the first stage of test started. The lamp was switched off, and the soil surface of each box was then ponded with 6 mm of constant water head for 1 minute. For a wetting event with a known ponding head and duration, a return period can be estimated through a Gumbel distribution (Gumbel, 1941). This distribution is a probability density function, of which the parameters have been calibrated by Lam and Leung (1995) using 100-year rainfall data collected in Hong Kong. Based on the statistical analyses, Intensity-Duration-Frequency (IDF) relationship is established and tabulated in DSD (2013) for general civil engineering design purposes. For the wetting event applied in this study (i.e., 6 mm in 1 minute), the return period can be estimated to be 100 years by using the IDF table. In the second stage, all boxes were left exposed in the plant room for 12 hours to study suction recovery after the wetting event. At both stages, the responses of suction at all four depths were recorded, while the bottom drainage holes of the three boxes remained open any for free drainage.

For the second series of tests conducted under light condition (i.e., boxes B_L, T1_L, T2_L and T3_L), identical test procedures were adopted, except that the lamp was switched on for controlling constant radiant energy (15.3 MJ m^{-2} d^{-1}) during the entire test.

After the two-stage test, SWRCs of bare and vegetated soil were measured using the transient-state method described by Ng and Leung (2012). A rigid cylindrical sampler with a diameter of 50 mm and a depth of 100 mm was used to excavate soil samples at the centre of each test box (with and without vegetation) for SWRC testing. The tree shoot above the soil surface was

removed from each vegetated box. All soil samples were water-saturated, following the typical test procedures adopted by Ng and Pang (2000). Both the upper and bottom sides of each soil sample were clamped with a water-saturated filter paper and a porous stone. Each sample was then submerged in de-aired water inside a desiccator, where a small amount of vacuum (i.e., < 2 kPa) was applied for 48 hours. The saturation process was considered to be completed when negligible amount of air bubbles was observed. Trial tests suggest that by adopting these procedures, the degree of saturation of each sample was as high as 98%. Each saturated sample was then exposed in the plant room for drying. During the process, the weight of each soil column was monitored by a high-resolution electronic balance for determining any change of volumetric water content (VWC). A tensiometer was installed at the mid-height to monitor the associated change in soil suction. The drying test was stopped when suction recorded by any tensiometer reached 80 kPa (i.e., limit of the working range of each tensiometer). Then, ponding was applied on the soil surface to undergo wetting process. Similarly, any changes in VWC and suction were determined, until all tensiometers recorded zero suction. A drying and wetting WRC was then obtained by directly relating VWC with suction. Two additional bare soil samples compacted at the identical dry density and dimensions were tested for SWRC, in order to check the repeatability of test results.

After each SWRC test, the biomass of shoot and roots in each vegetated soil sample (i.e., $0 - 30$ mm depth) were determined. For measuring the root biomass of each sample, the procedures were (i) to weight and oven-dry each soil sample at 60 $^{\circ}$C for 24 hours; (ii) to sieve away soil

particles with diameters larger than 2 mm; (iii) to collect any root retained on 2 mm and 0.841 mm

sieve considering the diameter of roots ranging from 1 to 2 mm; (iv) to repeat steps (ii) and (iii) until

no root was retained on the sieve; (v) to weight and determine the dry root biomass (Liang et al.,

1989). Identical procedures were adopted to determine the root biomass at deeper depth ranges of 30

– 70 mm and 70 – 100 mm.

2.6   *Observed properties of tree individuals*

Fig. 2 correlates the measured biomass of shoots and roots of the six tree individuals after testing. It

is evident that the tree individual having a higher shoot biomass has a higher root biomass. Based on

the dataset, almost a linear relationship between the biomass of shoots and roots is observed. Except

the box T3_L, all other data points are slightly below the 1:1 line, meaning that the root biomass of

these individuals is lower than the shoot biomass. The exceptional case for the box T3_L is

attributed to some existing plant variability, even though the tree individual in this particular test

box was growth and tested under the identical conditions to the other five tree individuals. Based on

the measurements from the six tree individuals, it is found that the average ratio of root biomass to

shoot biomass is about 1.22.

Fig. 3 depicts the measured profiles of root biomass along the root depth of all six tree

individuals. It should be noted that the data points at 15, 50 and 85 mm depths in the figure refer to

the total biomass of roots determined within the depth ranges of 0 – 30 mm, 30 – 70 mm and 70 –

100 mm, respectively. For the three boxes tested under dark condition, the root biomass in shallower

depths is generally higher than that in deeper depths. Similar shape of profile is observed for the other three boxes tested under light condition, but the magnitude at all three average depths is always higher due to the plant variability. The observed difference is the most significant in the shallowest depth.

2.7   *Soil water retention ability of vegetated soil*

Fig. 4(a) compares the measured drying SWRCs of bare soil and vegetated soil. The fitting equation proposed by van Genuchten (1980) was used to obtain a median, an upper and a lower bound of SWRCs (both drying and wetting) of both bare and vegetated soil. The fitting parameters (α, n and m, where m is set equal to $1 - 1/n$) are listed in Table 3. It can be seen that both the drying and wetting SWRCs obtained from the three bare soil samples are consistent with each other. As shown in Fig. 4(a), it can be identified that the air-entry value (AEV) of the bare soil is about 1 kPa, beyond which the VWC reduced substantially from about 34% to 10% at suction of 80 kPa. For the vegetated soil, some variability of SWRC existed because of the different root biomass (Table 2) of the six vegetation soil. Despite of the tree variability, it is evident that the AEV of vegetated soil (~3 – 4 kPa) is higher than that of the bare soil. As indicated by the fitting parameter, n, the desorption rate (i.e., amount of VWC reduction due to an increase in suction) of the bare and vegetated soil is similar. Based on the limited datasets obtained in this study, it appears that the roots could induce substantial change in the SWRC.

Along the wetting path (Fig. 4(b)), the increase in VWC in both bare and vegetated soil did

not follow the corresponding drying path, resulting in marked hydraulic hysteresis. The wetting

SWRCs of vegetated soil exhibited some fluctuation by ±5% due to the variability of tree root

biomass. Based on the repeated tests, it may be seen that the adsorption rate (i.e., amount of VWC

increase due to a decrease in suction) of vegetated soil is similar to that of the bare soil.

3.   Numerical modelling

The main purposes of the numerical analyses are (i) to justify the possibilities of the change of

suction responses due to the root-induced modification of SWRC (i.e., mechanism M1); and (ii) to

investigate whether tree LAI is sufficient to capture the effects of tree variability on suction

responses. A finite element software, HYDRUS-1D, was used to simulate isothermal water flow and

vapour flow in unsaturated, non-deformable, vegetated soil. It has been identified from various

experimental studies (Chiu and Ng, 2012; Leung and Ng, 2015) that densely-compacted decomposed

soil material with relatively high coarse content, like the CDG investigated in this study, exhibited

negligible volume change for suctions less than 100 kPa, which is the peak value observed in this

experiment (shown later). This is different from the study of clay materials reported by Navarro et al.

(2008). It is thus reasonable to assume the CDG to be rigid during water and vapour flow. In

HYDRUS, the following governing equation is adopted:

$$\frac{\partial(\theta_w + \theta_v)}{\partial t} = \frac{\partial}{\partial z}\left[\left(k_w(\psi) + k_v(\psi)\right)\left(\frac{\partial(\psi + z)}{\partial z}\right)\right] - S, \qquad \text{where } S = \alpha(\psi) \cdot G(\beta) \cdot PT \qquad (3)$$

where θ_w is volumetric liquid water content; θ_v is volumetric water vapour content; t is elapsed time;

z is the depth under consideration; ψ is suction; $k_w(\psi)$ is isothermal hydraulic conductivity of liquid

water; $k_v(\psi)$ is isothermal hydraulic conductivity of water vapour, which may be expressed as:

$$k_v(\psi) = \frac{D_v}{\rho_w} \rho_{vs} \frac{Mg}{RT} (RH) \tag{4}$$

where D_v is the diffusivity of water vapour, which is a function of air-filled porosity (or volumetric air content of soil) and air temperature T (which was maintained constant at 22.3 °C in this study); ρ_w is density of liquid water; ρ_{vs} is saturated vapour density; M is molecular weight of water (i.e., 0.018015 kg mol^{-1}); g is gravitational acceleration (i.e., 9.81 m s^{-2}); R is universal gas constant (i.e., 8.314 J mol^{-1} K^{-1}); and RH is relative humidity within soil pore, which is linked to suction through Kelvin equation.

The sink term, S, represents the volume of water transpired by the plant integrating over the entire root zone for a given time interval. The $\alpha(\psi)$ is to control the capability of root-water uptake when plant encounters stressed conditions. This includes (i) oxygen stress, when soil is too wet and plant would stop transpiring due to a lack of soil aeration; Dasberg and Bakker, 1970); (ii) water stress, when soil is too dry and plant has increased difficulties to extract soil moisture further; and (iii) plant wilt, when soil moisture is lower than a critical value. Based on these stressed conditions defined in $\alpha(\psi)$, actual transpiration (AT) could be determined. $G(\beta)$ depends on the distribution of root biomass, which reflects the ability of roots to extract soil moisture within a root zone for a given PT.

In total, 21 analyses were performed (Table 4), following the identical laboratory test conditions described above. Two analyses considered the responses of suction in bare soil, while the

remaining 19 investigated vegetated soil under different conditions. For the sake of discussion, a naming system for the simulation ID is defined. Each ID has three components; the first represents the type of soil being analysed (i.e., bare soil (*B*) or vegetated soil (*T1*, *T2* or *T3*) that has LAI of 1.6, 2.3 and 3.9, respectively); the second indicates the lighting condition (i.e., dark (*D*) or light (*L*)); and the last denotes the SWRC used (i.e., median (*M*), lower bound (*L*) or upper bound (U)). For example, the ID, *cT2_D_U* means that the analysis was conducted for vegetated soil having a tree LAI of 3.9 (i.e., *T2*) without the supply of light (i.e., *D*) using the upper bound SWRC (i.e., *U*).

3.1   *Input parameters for soil and tree*

For analysing transient seepage in unsaturated soil, SWRC and hydraulic conductivity function ($k(\psi)$), are needed to solve Eq (3). The measured wetting SWRCs of bare and vegetated soil, including the median, lower and upper bound curves (see Fig. 4(b)), were inputted. Based on the fitting coefficients of van Genuchten (1980)'s equation of each SWRC (Table 3) and saturated hydraulic conductivity (k_s; Table 4) measured by falling-head tests (ASTM, 2003), a $k_w(\psi)$ was estimated by the predictive equation suggested by van Genuchten (1980). In the analyses that modelled vegetated box (except *c_T3_D_M-no*), the two hydraulic properties of vegetated soil were specified in the top 100 mm within the root zone, while for depths below the root zone, the properties of bare soil were used. In simulation *c_T3_D_M-no*, the two hydraulic properties of bare soil were used for the entire depth. This simulation is a special case that aims to illustrate the effects of *not* considering mechanism M1 on suction response.

For each analysis of vegetated soil, two root parameters (α (ψ) and $G(\beta)$) are needed to model the tree root-water uptake, and hence to calculate any sink created by tree. For α (ψ), the relationship proposed by Feddes et al. (1978) was adopted, which has been commonly used for investigating various engineering problems in relation to soil-water-root interaction (Indraratna et al., 2006; Nyambayo and Potts, 2010). It was modelled that (i) the tree transpires only when soil suction is higher than 1 kPa as oxygen stress relieves (i.e., anaerobiosis point, ψ_{ap}) and lower than 1500 kPa before plant wilt (i.e., wilting point, $\psi_{wp,}$); and (ii) the ability of root-water uptake is maximum between 1 and 40 kPa (i.e., suction corresponding to the onset of water stress, ψ_{ws}), beyond which the transpiration reduces linearly to wilting point. Based on the measured distribution of root biomass shown in Fig. 3, a linear $G(\beta)$ is adopted. The $G(\beta)$ reduces from 1.0 at the soil surface to 0.0 at the tree root depth (i.e., at about 100 mm) linearly. This physically means that the ability of root-water uptake is the highest at the soil surface, and then decreases along depth due to the reduction of root biomass with increasing depth.

3.2   *Boundary and initial conditions*

For the soil-plant-atmosphere boundary condition at the surface of each bare and vegetated soil, the atmospheric parameters, including radiation, air temperature and RH, controlled in the plant room were specified. PE of the bare soil was calculated by Penman equation (i.e., Eq (1)), while for the case of vegetated soil, PET was calculated by Penman-Monteith equation (i.e., Eq (2)) and was then partitioned to PT and PE through the following equations using the Beer-Lambert law (Ritchie,

1972):

$$PT = PET\left(1 - e^{-k \cdot LAI}\right) \tag{5a}$$

$$PE = PET \cdot e^{-k \cdot LAI} \tag{5b}$$

where k is a constant that governs the radiation extinction by the tree leaves, and it typically ranges

from $0.5 - 0.75$. This parameter was calibrated to be 0.75 through a laboratory study conducted by

Garg (2015) for the same tree species in the same plant room investigated in this study. The

calculated PT would then be fed into the sink term for determining the AT, and the associated

induced suction. For the bottom boundary, a unit-gradient flux was specified to simulate the free

water drainage condition at the bottom of each test box. This physically means that the nodal

discharge flux at the bottom boundary of each model was fixed to be equal to $-k$ (ψ), according to

Darcy's law.

Based on the observation of the suction distribution measured before the two-stage tests, an

initially uniform suction of 35 and 40 kPa was specified along the depth of bare and vegetated soil,

respectively. Comparisons of measured and computed distribution of initial suction are given later.

4.   Interpretation of measured and computed results

4.1   *Effects of mechanism M1 on suction responses*

Fig. 5 compares the measured variations of suction with time between the bare soil (Box B_D) and

the three vegetated soil (Boxes T1_D, T2_D and T3_D), when they were all tested under dark

condition. At 80 mm depth within the root zone (Fig. 5(a)), the measured suctions reduced

significantly during the first four hours in both bare and vegetated soil due to ponding. It is evident that the amount of suction induced in the three vegetated soil after ponding was higher than that in the bare soil by up to 100%. During the subsequent drying period, only slight increases in suction are observed in both bare and vegetated soil. As no radiation was supplied for evaporation, the observed response was attributed to suction redistribution when the wetting front advanced to deeper depths. Despite of the tree variability, all three vegetated soil exhibited similar suction responses for the entire test. The numerical simulation generally showed consistent trends with the experimental data, especially during the wetting event. The discrepancies between measured and computed results during the drying period are mainly because of the negligence of hysteresis in the numerical analyses. At 210 mm depth below the root zone (Fig. 5(b)), suctions remained apparently unchanged in both the bare soil and the three vegetated soil. The suction difference between them was merely attributed to the difference of initial suction at the beginning of each test. From the numerical simulation, noticeable but slight decrease in suction is found in both bare and vegetated soil during drying, again because of the downward advancement of wetting front.

The measured suction profiles between the three vegetated soil in boxes T1_D, T2_D and T3_D are compared in Fig. 6(a). Within the root zone, the suction induced in all the vegetated soil was always higher than that in the bare soil. Under the dark testing condition, the radiation term PET_{rad} (Eq 2) was zero. Therefore, the aerodynamic term PER_{aero} is the only driver for ET to take place in vegetated soil. For the controlled constant air temperature of 22.3 °C and RH of 53% in the

plant room, it can be estimated that PET_{aero} for all three vegetated soil is also close to zero. This is because during the test, the plant room has almost zero wind speed that led to a high aerodynamic resistance (r_a in Eq 2) at leaf surface. As a result, the key factor that caused the higher induced suction in vegetated soil was not through tree ET (or M2), but was primarily attributed to the change of soil water retention capability induced by roots (i.e., M1). This is confirmed by the numerical simulations shown in Fig. 6(b). When mechanism M1 is not considered (i.e., using hydraulic properties of bare soil to model vegetated soil; see *cT3_D_M-no*), the computed suction in the vegetated soil is almost the same as that in the bare soil. In contrast, when this particular mechanism is taken into account (*cT3_D_M, cT3_D_L* and *cT3_D_U*), the computed suction bound in vegetated soil was much higher. Note that the shaded region represents the suction bound associated with the use of different wetting SWRCs (i.e., mean, lower bound and upper bound). Therefore, considering the root-induced modification of SWRC in vegetated soil is crucial for more correctly determining the suction responses.

4.2   *Combined effects of mechanisms M1 and M2 on suction responses*

Fig. 7(a) compares the responses of measured suction between the bare box B_L and the three vegetated boxes (T1_L, T2_L and T3_L), when they were all tested under light condition. Within the root zone, the suctions recorded in all three vegetated soil were always higher than that in the bare soil after the wetting event, similar to the observation found in the dark case (Fig. 6). However, the difference of induced suction between the bare and the vegetated soil was noticeably higher than

in the dark case, ranging between 18 to 26 kPa (i.e., 100% – 160%) due to tree variability. In the numerical simulations, although the computed suctions in all three vegetated soil are also significantly higher than that in bare soil, they are almost identical to each other, despite of the use of different LAI (i.e., 1.6 – 3.9; Table 4).

During the subsequent drying period, it is interesting to see from the experiments that suction at 80 mm depth in box T1_L reduced continuously, whereas the other two (T2_L and T3_L) exhibited substantial suction recovery after six hours. When compared the tree properties listed in Table 2, it might be identified that the higher the LAI of the tree individual, the greater the amount of suction recovered would be. Measurements from the quantum sensors suggested that that the tree individuals having LAI of 1.6, 2.3 and 3.9 intercepted 45%, 72% and 83% of radiant energy, respectively. However, from the numerical simulations where the effects of LAI on energy interception were considered, the computed suctions of the three vegetated soil did not response in the way observed in the experiments. They showed identical suction responses for the entire drying period. This implies that the variability of LAI could not be the only factor causing the different suction responses among the three vegetated soil. More discussion on the discrepancies between measured and computed results is given later.

On the contrary, at 210 mm depth (Fig. 7(b)), the responses of suction in both bare and vegetated soil were largely similar to the dark case, for both the measurements and simulations.

4.3   *Relative contribution of M1 and M2 on induced suction during wetting*

Fig. 8(a) compares the suction profiles of bare soil measured before and after ponding when tested under dark and light condition. It can be seen from the measurements that after the wetting event, the final suctions induced under the light condition at both 30 and 80 mm depth (5 and 10 kPa, respectively) were higher than those (4 and 8.5 kPa, respectively) under dark condition slightly, by not more than 2 kPa. Although this suction difference might be attributed to the difference of radiant energy received in the boxes B_L (15.3 MJ m^{-2} d^{-1}) and B_D (0 MJ m^{-2} d^{-1}), such marginal difference may be apparent because it is comparable with the accuracy of tensiometer (± 1 kPa). This is confirmed by the numerical simulations from *cB_D* and *cB_T*. Even though the evaporation process was considered, the computed suction profiles between these two cases are almost identical after the wetting event.

In order to investigate the relative importance of the two hydrological mechanisms on suction responses, the results of each pair of vegetated boxes tested under dark (i.e., M1 only) and light (i.e., M1 + M2) condition are compared. To isolate any effects of different values of LAI due to tree variability, the comparisons are presented in three separate figures by grouping T1_D and T1_L in Fig. 8(b), T2_D and T2_L in Fig. 8(c), and T3_D and T3_L in Fig. 8(d). The suction responses in each figure are therefore compared under a similar LAI. For the vegetated soil having LAI of about 1.6 (Fig. 8(b)), the supply of light did not seem to have significant effects as the magnitude of suction induced after rainfall was similar between the dark and light case. When the LAI of the tree individual increased from 1.6 to 3.9, the measured difference of suction within the

root zone between the dark and light case increased by almost 300%. This is, however, not found from the numerical simulations. The computed suction profiles between the dark and light case are the same, regardless of the value of LAI being considered.

To further interpret the suction responses during the wetting event, the computed cumulative infiltration in all boxes at one hour after the end of ponding is compared in Fig. 9, based on the water balance calculation performed in the numerical simulations. The computed actual evaporation (AE; for bare soil) and actual transpiration (AT; for vegetated soil) are also shown. For the bare soil, it is found that the volume of water infiltrated (~5.7 mm) is identical in the dark and light cases, because they have the same water storage capacity when the same SWRC was used in these two analyses. In the light case, an AE of about 0.1 mm is resulted due to the interception of radiant energy at the soil surface. As the soil moisture loss through evaporation is 1.7% of the cumulative infiltration only, the AE has negligible effects on suction responses. This thus led to the almost identical computed suction profiles between the dark and light case in Fig. 8(a).

For the analyses of the three vegetated soil in dark condition (Fig. 9), the cumulative volume of water infiltrated is higher than that in the bare soil, by about 0.2 mm. This is attributed to the increased water storage capacity of the vegetated soil induced by roots (Fig. 4). Since no radiation is supplied in these three cases, no water was loss through tree transpiration (i.e., AT = 0). This evidences that the observed difference of suction responses between the bare and vegetated soil in the dark condition (Figs 5 and 6) is primarily attributed to mechanism M1. When radiant energy is

available in the light case, the cumulative volume of water infiltrated is identical to that in the dark

case (Fig. 9). It can be seen that the AT is higher when the tree LAI is higher because of higher

percentage of energy interception. The remaining radiant energy that is not intercepted falls on soil

surface for AE. Nonetheless, the actual ET (i.e., AET = AT + AE) is identical in all three cases. This

explains why the computed suctions are identical after the wetting event (see Figs 7 and 8). The

AET in the three vegetated soil cases is less than 2% of the volume of water infiltrated. This

suggests that even with the supply of light, mechanism M2 did not help induce very significant

amount of suction during the wetting event. Instead, M1 appears to be a more dominant mechanism

that results in the observed differences of suction responses between the bare and vegetated soil,

regardless of whether the wetting event happened under light or dark condition.

4.4   *Relative contribution of M1 and M2 on suction recovery during drying*

Comparisons of suction profiles of the bare soil before and after 12 hours of drying period under

dark and light condition are shown in Fig. 10, for both laboratory measurements and numerical

simulations. Note that the initial suction profiles before drying are identical to the final suction

profiles after ponding shown in Fig. 8. As can be seen in Fig. 10, both measured and computed

suctions at all depths showed substantial reduction when the drying event took place under dark

condition. This is attributed to the downward advancement of wetting front resulted from the

previous wetting event. In the light case, although suctions below 80 mm depth also showed

substantial reduction like the dark case, it is evident that there were substantial suction increases in

the top 100 mm due to the additional evaporation process.

For the vegetated soil having the three different values of LAI tested under the dark condition, the measured responses of suction were largely similar to each other (Figs 11(a), (c) and (e)). This is because LAI has no effect when no radiant energy was supplied for tree leaf interception. It can be seen that the suction at 30 mm depth in all three vegetated soil increased by about 120% after 12 hours of drying period. Similar observation is found from the numerical simulations (Figs 11(b), (d) and (f)). This is merely the redistribution of suction as wetting front advanced downwards. Under the light case, suction recovery is also observed in all three cases, but the amount of suction increases were much higher than that in the dark case. From the experiments, it appears that the magnitude of final suction recovered within the root zone was higher, when LAI was higher. Such correlation is, however, not found from the simulations. The computed suction profiles in all light cases are identical, even though the simulations have considered the tree variability through LAI. This suggests that considering LAI alone is not sufficient to capture the tree variability. Some other tree characteristics such as hydraulic conductivity of roots and xylem and leaf-atmosphere surface resistance might be the potential factors causing tree variability. However, these factors in microscopic scale could not be considered appropriately by using the relatively simple macroscopic root-water uptake model (i.e., through a general sink term) in HYDRUS.

Computed water balance during the drying event is investigated in Fig. 12. For the bare soil, only the analysis for the light case showed significant amount of AE of 1.2 mm after drying. The

associated loss of soil moisture thus caused higher induced suction in simulation *cB_L*, as compared to *cB_D* (Fig. 10). For the vegetated soil analysed under dark condition, no AT took place (Fig. 12). M1 is thus the major mechanism causing the higher suction induced in the vegetated soil than in bare soil (compare Figs 10 and 11). In contrast, when radiant energy is considered in other three vegetated soil cases, *cT1_L_M*, *cT2_L_M* and *cT3_L_M*, much more significant AT and AE are resulted. Although the proportion of AT and AE is different between the three simulations, the AET (i.e., AT + AE) is the same. This explains why the computed suctions between these three vegetated soil cases are identical in Figs 7 and 11. However, it is interesting to note that even though the AET of the three vegetated soil is identical to the AE of the bare soil in the case *cB_L*, the suction induced in the vegetated soil was still higher than that in the bare soil (Figs 10 and 11), as consistently found in both the experiments and simulations. This is because the soil drying process through AT took place within the entire root zone in the top 100 mm of vegetated soil, whereas that through AE was at the soil surface of bare soil only.

5.   Summary and conclusions

Based on two series of laboratory testing together with 21 numerical simulations of transient seepage, this study investigates root-induced change in water retention ability (mechanism M1) and its effect on suction responses. Effects of this hydrological mechanism M1 and another well-recognised mechanism, plant ET and root-water uptake (mechanism M2), on induced suction are

quantified, compared and discussed. Experiments were conducted on soil vegetated with a selected tree species, *Schefflera heptaphylla*, under dark and light condition in an atmosphere-controlled plant room. To take into account the effects of tree variability, six replicates of tree individuals with the same age were tested. Drying and wetting SWRCs of six vegetated soils were measured to provide experimental evidence to support M1. Properties of each tree individual that could affect the ability of root-water uptake (i.e., M2) were also determined, including LAI and the distribution of root biomass.

It is revealed that the tree roots induced substantial change of the SWRCs (i.e., M1). Comparison of SWRCs of bare and vegetated soil showed that the roots induced increases in AEV from 1 to 4 kPa, as well as the size of hysteresis loop. After subjecting to a ponding event with an equivalent return period of 100 years under dark environment, suction induced within the root zone of vegetated soil was 100% higher than that in bare soil, consistently found in both the experiments and the numerical analyses. This suggests that even though plant ET and root-water uptake (i.e., M2) are not considered, vegetated soil could still be able to preserve higher suction than bare soil during a wetting event through the root-induced modification of SWRC (i.e., M1).

When the wetting event was conducted under the supply of light, vegetated soil also induced higher suction than bare soil. However, the suction difference was much larger than that in the dark case, ranging between 100% and 160% due to the tree variability. It is revealed from the numerical analyses that tree LAI is not sufficient to capture the variability of the suction responses.

Furthermore, it is shown by the computed water balance that the AET is minimal during the wetting event, even though radiation was supplied. The soil moisture loss through AET was only 1.7% of the total volume of water infiltrated. This suggests that the observed higher suction may be attributed to the change of SWRC induced by roots (i.e., M1) more dominantly, rather than the result of AET and root-water uptake through M2.

Acknowledgements

References

Allen, R.G., Pereira, L.S., Raes, D., Smith, M., 1998. Crop evapotranspiration. Guidelines for computing crop water requirements. Irrigation and Drainage Paper 56. Rome, Italy, FAO.

ASTM D5084, 2003. Standard test methods for measurement of hydraulic conductivity of saturated porous materials using a flexible wall permeameter. American Society for Testing and Materials International, West Conshohocken, PA

Biddle, P.G., 1983. Patterns of soil drying and moisture deficit in the vicinity of trees on clay soils.

Géotechnique 33 (2), 107–126.

Blight, G.E., 2003. The vadose-zone soil–water balance and transpiration rates of vegetation. Géotechnique 53 (1), 55–64.

Carrow, R.N., 1996. Drought resistance aspects of turfgrasses in the southeast: Root-shoot responses. Crop Science 36 (3), 687-694.

Chiu, C.F., Ng, C.W.W., 2012. Coupled water retention and shrinkage properties of a compacted silt under isotopic and deviatoric stress paths. Canadian Geotechnical Journal 49, 928 – 938.

Dasberg, S., Bakker, J.W., 1970. Characterizing soil aeration under changing soil moisture conditions for bean growth. Agronomy Journal 62, 689–692.

DSD, 2013. Stormwater drainage manual – planning design and management. Drainage Services Department (DSD), Government of the Hong Kong Special Administrative Region

Feddes, R.A., Kowalik, P., Kolinska-Malinka, K., Zaradny, H., 1976. Simulation of field water uptake by plants using a soil water dependent root extraction function. Journal of Hydrology 31 (1), 13-26

Frodin, D.G., Lowry, I.I., Porter, P., Plunkett, G.M., 2010. Schefflera (Araliaceae): taxonomic history, overview and progress. Plant Diversity and Evolution 128 (3-4), 3-4.

Gan, J.K.M, Fredlund, D.G., Rahardjo, H., 1988. Determination of the shear strength parameters of an unsaturated soil using the direct shear test. Canadian Geotechnical Journal 25 (3), 500–510.

Garg, A. 2015. *Effects of vegetation types and characteristics on induced soil suction*. PhD Thesis.

The Hong Kong University of Science and Technology, Hong Kong.

GEO, 2011. Technical Guidelines on Landscape Treatment for Slopes (GEO publication No. 1/2011). Geotechnical Engineering Office (GEO), Civil Engineering and Development Department, Government of the Hong Kong Special Administrative Region.

Grayston, S.J., Vaughan, D., Jones, D., 1997. Rhizosphere carbon flow in trees, in comparison with annual plants: the importance of root exudation and its impact on microbial activity and nutrient availability. Applied Soil Ecology 5 (1), 29-56.

Gumbel, E.J. 1941. The return period of flood flows. The annals of mathematical statistics 12 (2), 163-190

Hau, B.C., Corlett, R.T. 2003. Factors affecting the early survival and growth of native tree seedlings planted on a degraded hillside grassland in Hong Kong, China. Restoration Ecology 11 (4), 483-488.

Hemmati, S., Gatmin, B., Cui, Y.J., Vincent, M., 2012. Thermo-hydro-mechanical modelling of soil settlements induced by soil-vegetation-atmosphere interactions. Engineering Geology 139-140, 1-16.

Hu, L., Wang, Z., Du, H., Huang, B., 2010. Differential accumulation of dehydrins in response to water stress for hybrid and common bermudagrass genotypes differing in drought tolerance. Journal of Plant Physiology 167 (2), 103-109.

Indraratna, B, Fatahi, B., Khabbaz, H., 2006. Numerical analysis of matric suction effects of tree

roots. Proceedings of ICE, Geotechnical Engineering 159 (2), 77–90.

Krahn, J., Fredlund, D.G., 1972. On total, matric and osmotic suction. Soil Science 114 (5), 339-348.

Ladd, R.S., 1978. Preparing specimens using undercompaction. Geotechnical Testing Journal 1 (1), 16–23.

Lam, C.C., Leung, Y.K., 1995. Extreme rainfall statistics and design rainstorm profiles at selected locations in Hong Kong. Technical Note, No. 86. Royal Observatory, Hong Kong.

Liang, Y.M., Hazlett, D.L., Lauenroth, W.K., 1989. Biomass dynamics and water use efficiencies of five plant communities in the shortgrass steppe. Oecologia 80 (2), 148-153.

Lim, T.T., Rahardjo, H., Chang, M.F., Fredlund, D.G., 1996. Effect of rainfall on matric suctions in a residual soil slope. Canadian Geotechnical Journal 33 (4), 618–628.

Leung, A.K., 2014. Grass evapotranspiration-induced suction in slope: case study. Proceedings of Institute of Civil Engineers, Environmental Geotechnics. (In press) doi: 10.1680/envgeo.14.00010

Leung, A.K., Ng, C.W.W., 2013a. Seasonal movement and groundwater flow mechanism in an unsaturated saprolitic hillslope. Landslides 10 (4), 455–467.

Leung, A.K., Ng, C.W.W., 2013b. Analyses of groundwater flow and plant evapotranspiration in a vegetated soil slope. Canadian Geotechnical Journal 50 (12), 1204–1218.

Leung, A.K., Ng, C.W.W., 2015. Field investigation of deformation characteristics and stress mobilisation of a soil slope. Landslides. In press. DOI: 10.1007/s10346-015-0561-x

Navarro, V., Yustres, A., Candel, M. and García, B., 2008. Soil air compression in clays during flood

irrigation. European Journal of Soil Science 59, 799-806.

Ng, C.W.W., Leung, A.K., 2012. Measurements of drying and wetting permeability functions using a new stress-controllable soil column. Journal of Geotechnical and Geoenvironmental Engineering, ASCE 138 (1), 58–65.

Ng, C.W.W., Pang, Y.W., 2000. Experimental investigations of the soil-water characteristics of a volcanic soil. Canadian Geotechnical Journal 37 (6), 1252–1264.

Ng, C.W.W, Leung, A.K., Woon, K.X., 2014. Effects of soil density on grass-induced suction distributions in compacted soil subjected to rainfall. Canadian Geotechnical Journal 51 (3), 311–321.

Ng, C.W.W., Woon, K.X., Leung, A.K., Chu, L.M., 2013. Experimental investigation of induced suction distribution in a grass-covered soil. Ecological Engineering 52, 219–223.

Nyambayo, V.P., Potts, D.M., 2010. Numerical simulation of evapotranspiration using a root water uptake model. Computers and Geotechnics 37, 175–186.

Penman, H.L., 1948. Natural evaporation from open water, bare soil and grass. Proceedings of Royal Society of London Series A 193, 120–146.

Rahardjo, H., Satyanaga, A., Leong, E.C., Santoso, V.A., Ng, Y.S., 2014. Performance of an instrumented slope covered with shrubs and deep-rooted grass. Canadian Geotechnical Journal 54 (3), 417–425.

Ritchie, J.T., 1972. Model for predicting evaporation from a row crop with incomplete cover. Water

Resources Research 8 (5), 1204–1213.

Roberts, J., 2000. The influence of physical and physiological characteristics of vegetation on their hydrological response. Hydrological Processes 14, 2885-2901.

Romero, E., Gens, A., Lloret, A., 1999. Water permeability, water retention and microstructure of unsaturated compacted boom clay. Engineering Geology 54 (1–2), 117–127.

Scanlan, C.A., Hinz, C., 2010. Insight into the processes and effects of rootinduced changes to soil hydraulic properties. In 19th World Congress of Soil Science, Soil Solutions for a Changing World, Brisbane, Australia, 1– 6 August 2010. pp. 41– 44.

Scholl, P., Leitner, D., Kammerer, G., Loiskandl, W., Kaul, H-P., Bodner, G., 2014. Root induced changes of effective 1D hydraulic properties in a soil column. Plant and Soil 381 (1-2), 193–213.

Simon, A., Collison, A., 2002. Quantifying the mechanical and hydrologic effects of riparian vegetation on streambank stability. Earth Surface Processes and Landform 27 (5), 527 – 546.

Smethurst, J.A., Clarke, D., Powrie, W., 2006. Seasonal changes in pore water pressure in a grass-covered cut slope in London clay. Geotechnique 56 (8), 523–537.

Taha, H., Akbari, H., Rosenfeld, A., 1988. Residential Cooling Loads and the Urban Heat Island: the Effects of Albedo. Building and Environment 23 (4), 271–283.

Traoré, O., Groleau-Renaud, V., Plantureux, S., Tubeileh, A., Boeuf-Tremblay, V., 2000. Effect of root mucilage and modelled root exudates on soil structure. European Journal of Soil Science 51 (4), 575–581.

Taleisnik, E., Peyrano, G., Cordoba, A., Arias, C., 1999. Water retention capacity in root segments differing in the degree of exodermis development. Annals of Botany 83 (1), 19-27.

van Genuchten, M.T., 1980. A closed-form equation for predicting the hydraulic conductivity of unsaturated soils. Soil Science Society of American Journal 44 (5), 892–898.

Veihmeyer, F.J., Hendrickson, A., 1931. The moisture equivalent as a measure of the field capacity of soils. Soil Science 32, 181 – 193.

Vetterlein, D., Marschner, H., Horn, R., 1993. Microtensiometer technique for in situ measurement of soil matric potential and root water extraction from a sandy soil. Plant and Soil 149 (2), 263-273.

Wang, D., Kang, Y., Wan, S., 2006. Effect of soil matric potential on tomato yield and water use under drip irrigation condition. Agricultural Water Management 87 (2), 180-186.

Wang, Z., Feyen, J., Nielsen, D.R., Van Genuchten, M.T., 1997. Two-phase flow infiltration equations accounting for air entrapment effects. Water Resources Research 33, 2759-2767.

Wang, Z., Feyen J., Van Genuchten M.T., Nielsen, D.R., 1998. Air entrapment effects on infiltration rate and flow instability. Water Resources Research 34, 213-222.

Zhang, Y., Kendy, E., Qiang, Y., Liu, C., Shen, Y., Sun, H., 2004. Effect of soil water deficit on evapotranspiration, crop yield, and water use efficiency in the North China Plain. Agricultural Water Management 64 (2), 107–122.

LIST OF CAPTIONS

Table caption

Table 1. A summary of numeric values of each parameter for Penman equation and Penman-Monteith equation for calculating PE and PET

Table 2. A summary of measured properties of the six tree individuals

Table 3. A summary of fitting coefficients for SWRCs using van Genuchten (1980) equation

Table 4. A summary of numerical analysis plan

Figure captions

Fig. 1. Overview of the experimental setup and instrumentation of a typical vegetated box

Fig. 2. Relationship between shoot biomass and root biomass of the six vegetated soil samples

Fig. 3. Distributions of root biomass of the six vegetated soil samples

Fig. 4. Comparison of (a) drying SWRCs and (b) wetting SWRCs between bare and vegetated soil samples

Fig. 5. Measured and computed variations of suction with time for bare and vegetated soil tested in dark condition (a) at 80 mm depth within the root zone and (b) at 210 mm depth below the root zone

Fig. 6. Effects of mechanism M1 on the response of suction profiles when tested under dark condition (a) measurements and (b) simulations

Fig. 7. Measured and computed variations of suction with time for bare and vegetated soil tested in light condition (a) at 80 mm depth within the root zone and (b) at 210 mm depth below the root zone

Fig. 8. Measured and computed suction profiles in (a) bare soil and vegetated soil with LAI of (b) 1.61 − 1.63, (c) 2.29 − 2.34, and (d) 3.92 − 3.97 when subjected to ponding under dark and light condition

Fig. 9. Computed water balance in bare and vegetated boxes at one hour after the end of ponding

Fig. 10. Measured and computed suction profiles of bare soil when subjected to drying under dark and light condition

Fig. 11. Measured ((a), (b), (c)) and computed ((d), (e), (f)) suction profiles of vegetated soil with LAI of 1.61 – 1.63, 2.29 – 2.34 and 3.92 – 3.97 when subjected to 12 hours of drying period under dark and light condition

Fig. 12. Computed water balance in bare and vegetated soil after 12 hours of drying period

Table 1

A summary of numeric values of each parameter for Penman equation and Penman-Monteith equation for calculating PE and PET

Parameters	Value
Slope of vapour pressure curve, Δ	0.164 kPa $^{\circ}$C^{-1}
Radiant energy, R_n	15.3 MJ m^{-2} d^{-1}
Soil heat flux density, G_s	Assumed negligible as the magnitude is far lower than R_n
Latent heat of vaporisation, λ	2.45 MJ kg^{-1}
Psychometric constant, γ	0.0674 kPa $^{\circ}$C^{-1}
Relative humidity, e_a/e_s	53%
Air temperature	22.3 $^{\circ}$C
Saturated vapour pressure, e_s	2.69 kPa
Actual vapour pressure, e_a	1.43 kPa
Wind speed, u	0 m s^{-1}
Air density, ρ	0.001195 kg m^{-3}
Specific heat of moist air, c_p	1.013 kJ kg^{-1} $^{\circ}$C^{-1}
Canopy resistance, r_c	Depending on LAI 125 s m^{-1}, when LAI = 1.6 86.96 s m^{-1}, when LAI = 2.3 51.28 s m^{-1}, when LAI = 3.9
Aerodynamic resistance, r_a	47.98 s m^{-1}, for a given average shoot height of 425 mm

Table 2

A summary of measured properties of the six tree individuals

Tree properties	Box identity						Mean	S.D.
	T1_D	T2_D	T3_D	T1_L	T2_L	T3_L		
Shoot height (mm)	410	418	435	420	424	443	425	12
Canopy diameter (mm)	185	175	190	204	215	210	196.5	15.6
Total shoot biomass (g)	7.1	8.4	14.2	9.4	11.2	16.3	11.1	3.55
Leaf Area Index (LAI)	1.61	2.29	3.92	1.63	2.34	3.97	2.62	1.07
Basal diameter (mm)	6	6	8	8	10	11	8.17	2.04
Root depth (mm)	97	101	106	103	104	110	103.5	4.41
Total root biomass (g)	5.3	6.4	12.1	7.4	10.2	17.2	9.77	4.42

Note: S.D. stands for standard deviation

Table 3

A summary of fitting coefficients for SWRCs using van Genuchten (1980) equation

Soil type		Drying SWRC					Wetting SWRC				
		θ_s [m³/m⁻³]	θ_r [m³/m⁻³]	α [m⁻¹]	n [-]	m [-]	θ_s [m³/m⁻³]	θ_r [m³/m⁻³]	α [m⁻¹]	n [-]	m [-]
Bare soil		0.345	0.01	2.2	1.52	0.342	0.23	0.01	1.2	1.58	0.367
Vegetated soil	Lower bound	0.330	0.01	1.8	1.4	0.286	0.255	0.01	0.8	1.68	0.405
	Median	0.350	0.01	1.5	1.42	0.296	0.275	0.01	0.8	1.5	0.333
	Upper bound	0.365	0.01	1.0	1.5	0.333	0.295	0.01	0.8	1.46	0.315

Note: The parameter *m* is set equal to *1 – 1/n* (van Genuchten, 1980)

Table 4.
A summary of numerical analysis plan

Simulation ID*	Soil** α [m⁻¹]	n [-]	θ_s [m³/m³]	θ_r [m³/m³]	k_s (m/s)	Root*** ψ_ap [kPa]	ψ_ws [kPa]	ψ_w [kPa]	Initial suction [kPa]	R_n [MJ/m²/d]	T [°C]	RH [%]	LAI [-]	Bottom boundary
cB_D	1.2	1.58	0.23	0.01	1.7×10^{-7}	-	-	-	35				-	
cT1_D_M										0			1.6	
cT2_D_M	0.8	1.5	0.275	0.01	5.79×10^{-8}	1	40	1500	40				2.3	
cT3_D_M													3.9	
cB_L	1.2	1.58	0.23	0.01	1.7×10^{-7}	-	-	-	35				-	
cT1_L_M													1.6	
cT2_L_M	0.8	1.5	0.275	0.01	5.79×10^{-8}					15.3			2.3	
cT3_L_M													3.9	
cT3_L_M-no	1.2	1.58	0.23	0.01	1.7×10^{-7}						22	53	3.9	Unit gradient flow
cT1_D_L													1.6	
cT2_D_L										0			2.3	
cT3_D_L													3.9	
cT1_L_L	0.8	1.68	0.255	0.01		1	40	1500	40				1.6	
cT2_L_L										15.3			2.3	
cT3_L_L					5.79×10^{-8}								3.9	
cT1_D_U													1.6	
cT2_D_U										0			2.3	
cT3_D_U													3.9	
cT1_L_U	0.8	1.46	0.295	0.01									1.6	
cT2_L_U										15.3			2.3	
cT3_L_U													3.9	

* The first character denotes Bare (B) or Vegetated (T) soil; the second characterizes Dark (D) or Light (L) test condition; and the last represents Median (M), Lower (L) or Upper (U) bound of soil water retention curves used.

**Except *cT3_L_M-no*, the input soil parameters for vegetated soil were only applied within the root zone, while the parameters from bare soil were used below the root zone.

*** The parameters for root-water uptake model are taken from Feddes et al. (1976)
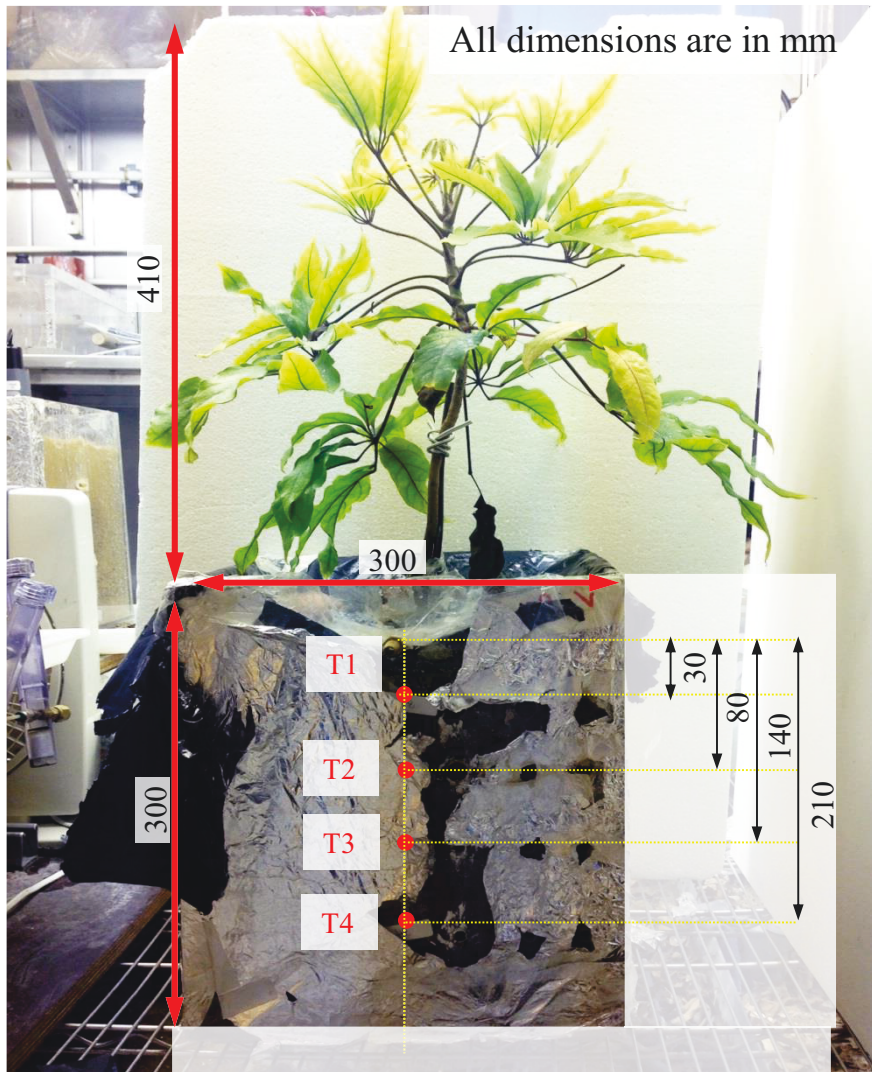
Fig. 1. Overview of the experimental setup and instrumentation of a typical vegetated box
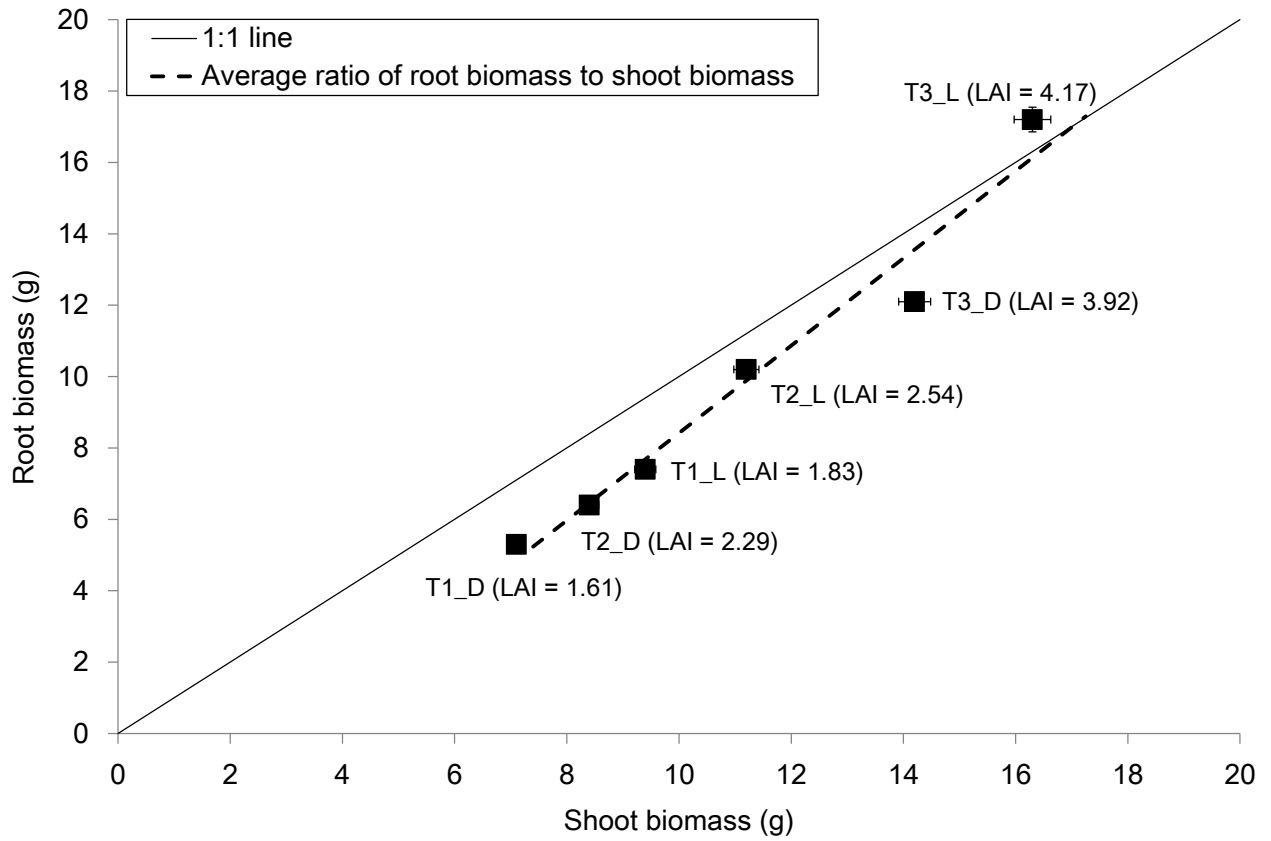
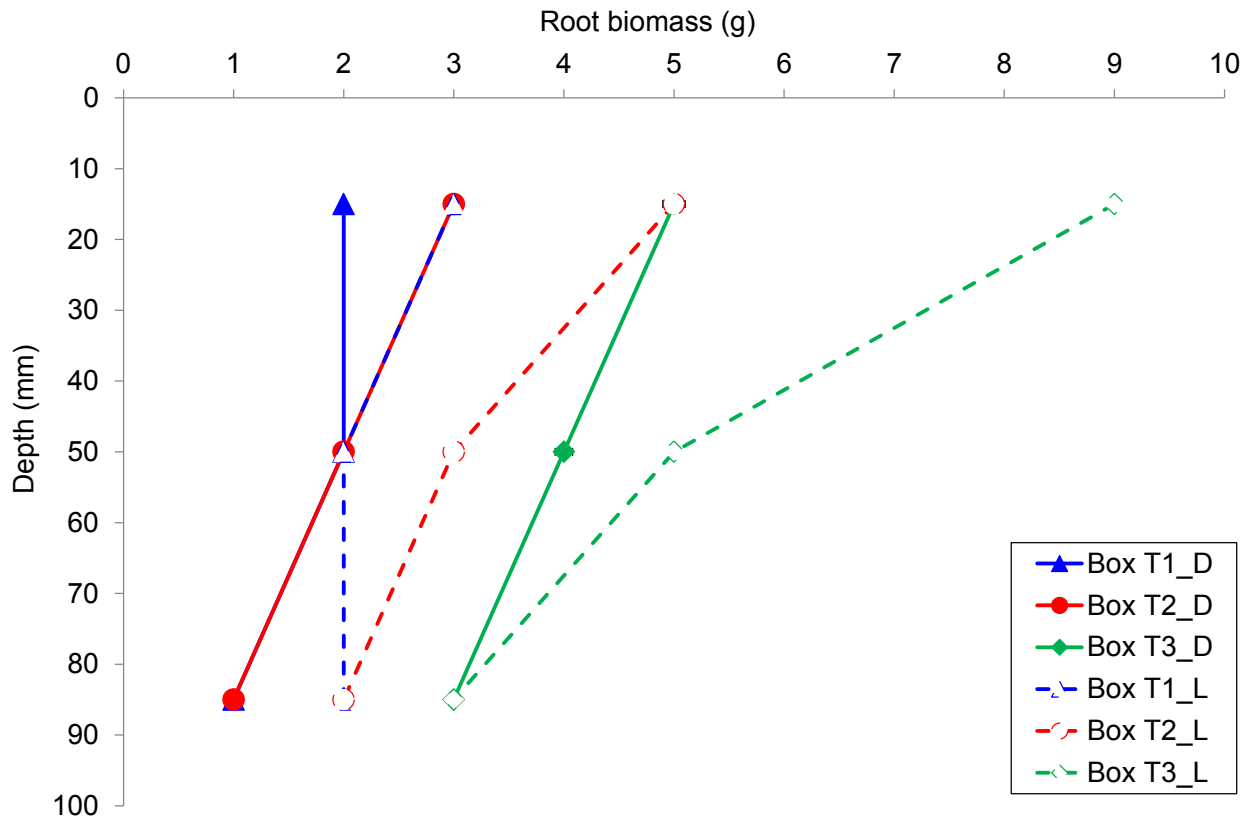**Fig. 2.** Relationship between shoot biomass and root biomass of the six vegetated soil samples

Fig. 3. Distributions of root biomass of the six vegetated soil samples
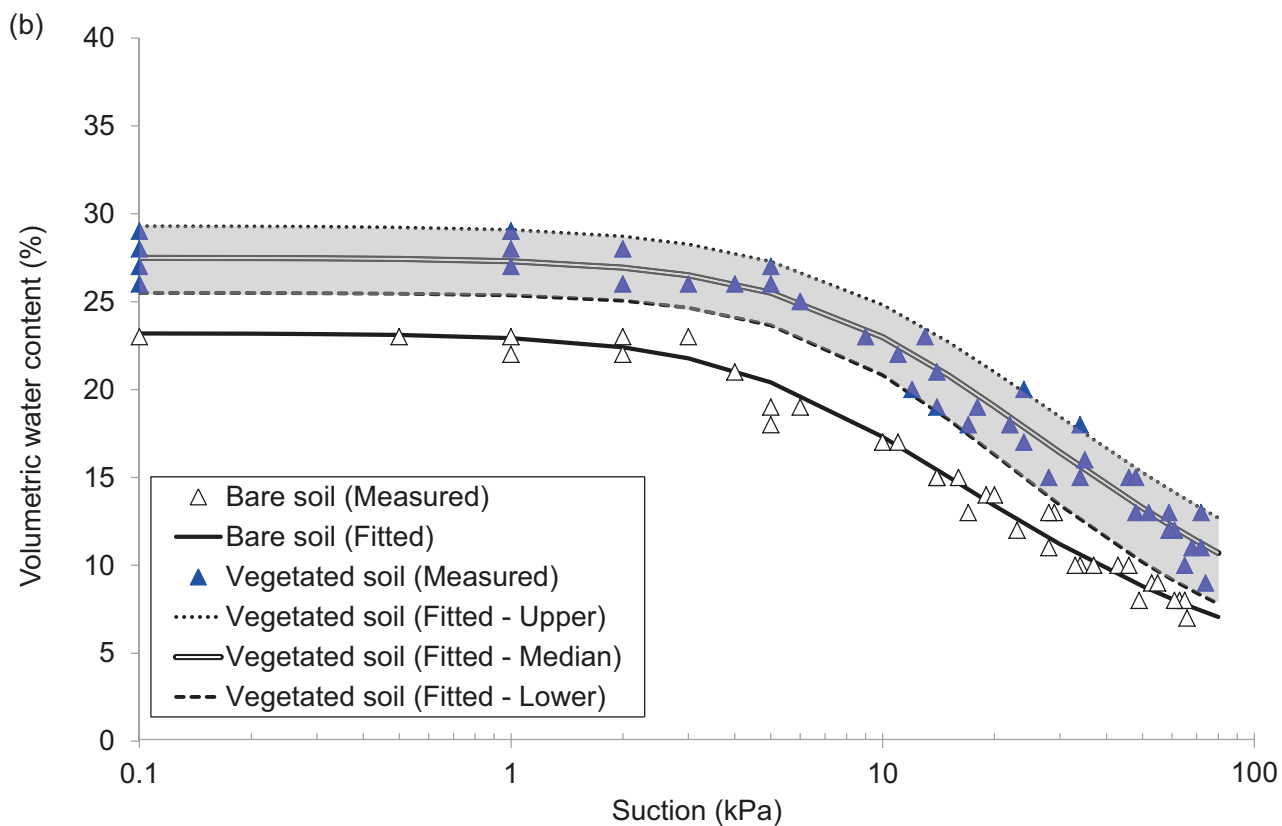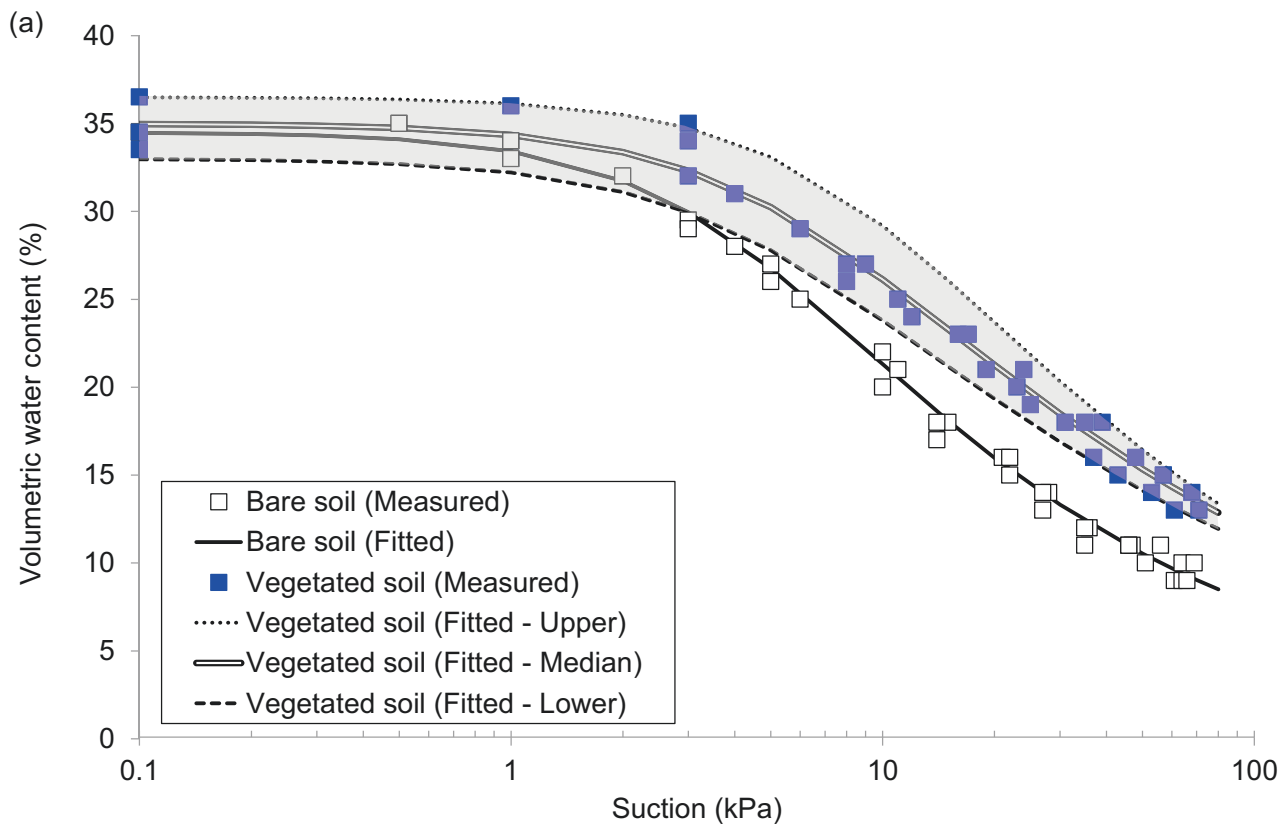
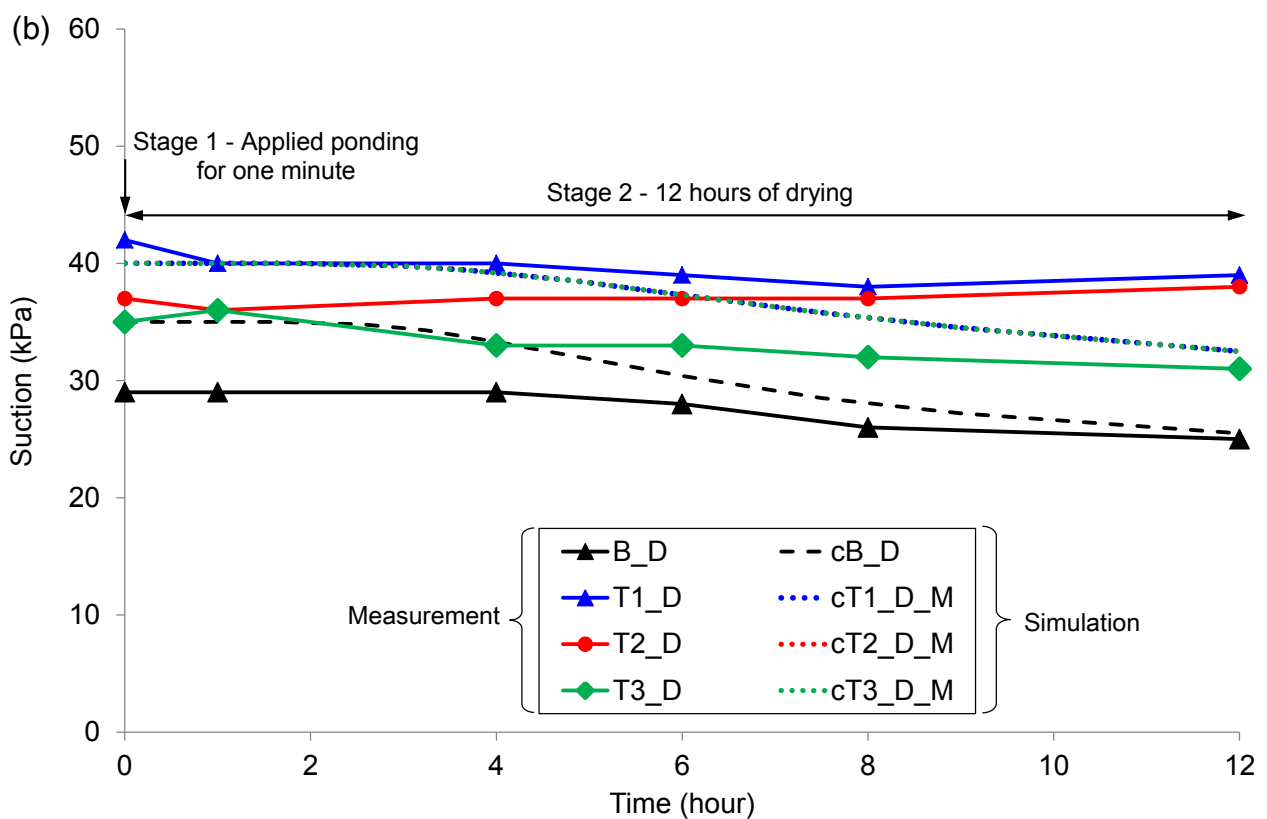**Fig. 4.** Comparison of (a) drying SWRCs and (b) wetting SWRCs between bare and vegetated soil sampels

Fig. 5. Measured and computed variations of suction with time for bare and vegetated soil tested in dark condition (a) at 80 mm depth within the root zone and (b) at 210 mm depth below the root zone
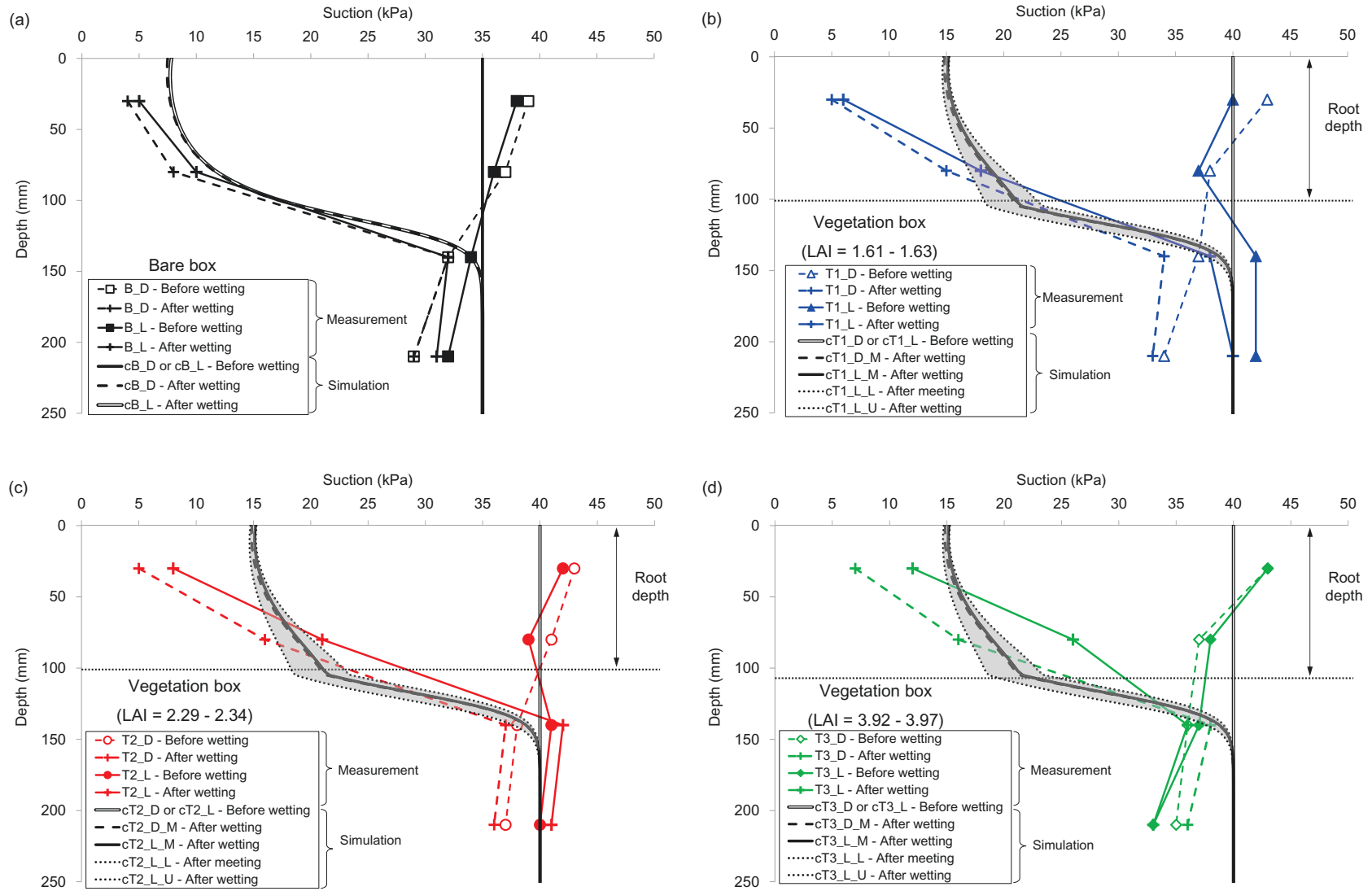
Fig. 6. Effects of mechanism M1 on the response of suction profiles when tested under dark condition (a) measurements and (b) simulations

Fig. 7. Measured and computed variations of suction with time for bare and vegetated soil tested in light condition (a) at 80 mm depth within the root zone and (b) at 210 mm depth below the root zone

Fig. 8. Measured and computed suction profiles in (a) bare soil and vegetated soil with LAI of (b) 1.61 – 1.63, (c) 2.29 – 2.34, and (d) 3.92 – 3.97 when subjected to ponding under dark and light condition

Fig. 9. Computed water balance in bare and vegetated boxes at one hour after the end of ponding
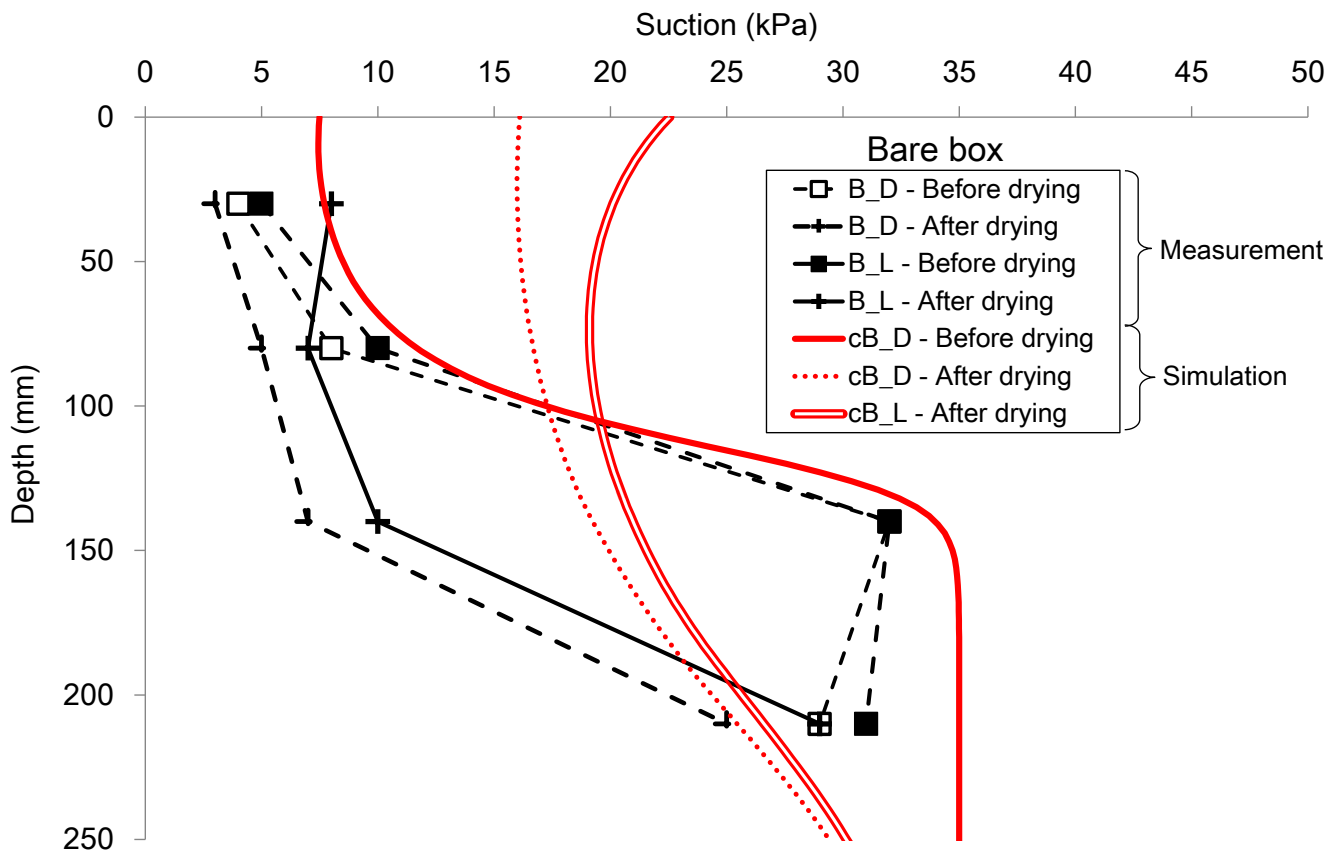
Fig. 10. Measured and computed suction profiles of bare soil when subjected to drying under dark and light condition
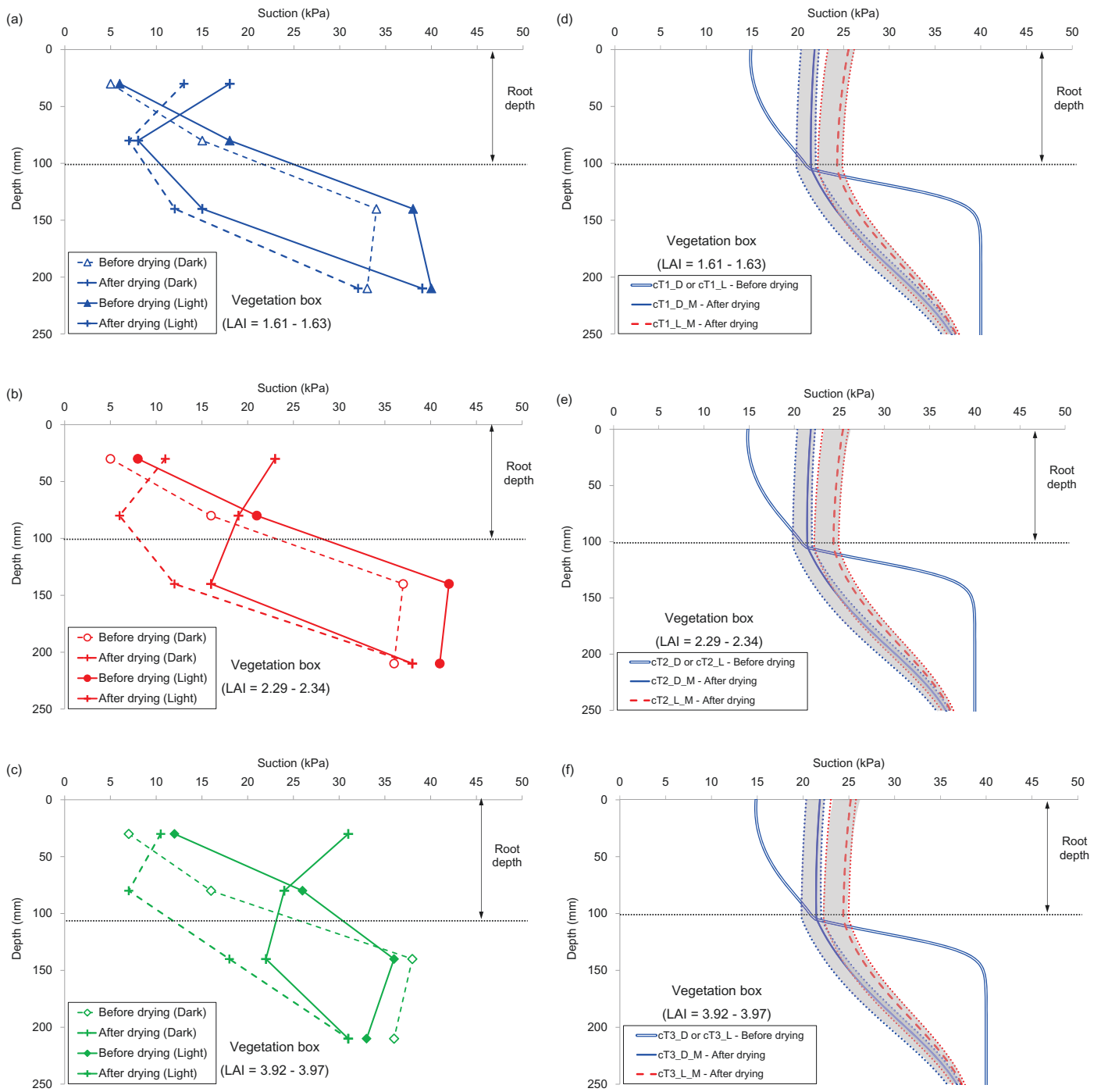
Fig. 11. Measured ((a), (b), (c)) and computed ((d), (e), (f)) suction profiles of vegetated soil with LAI of 1.61 – 1.63, 2.29 – 2.34 and 3.92 – 3.97 when subjected to 12 hours of drying period under dark and light condition
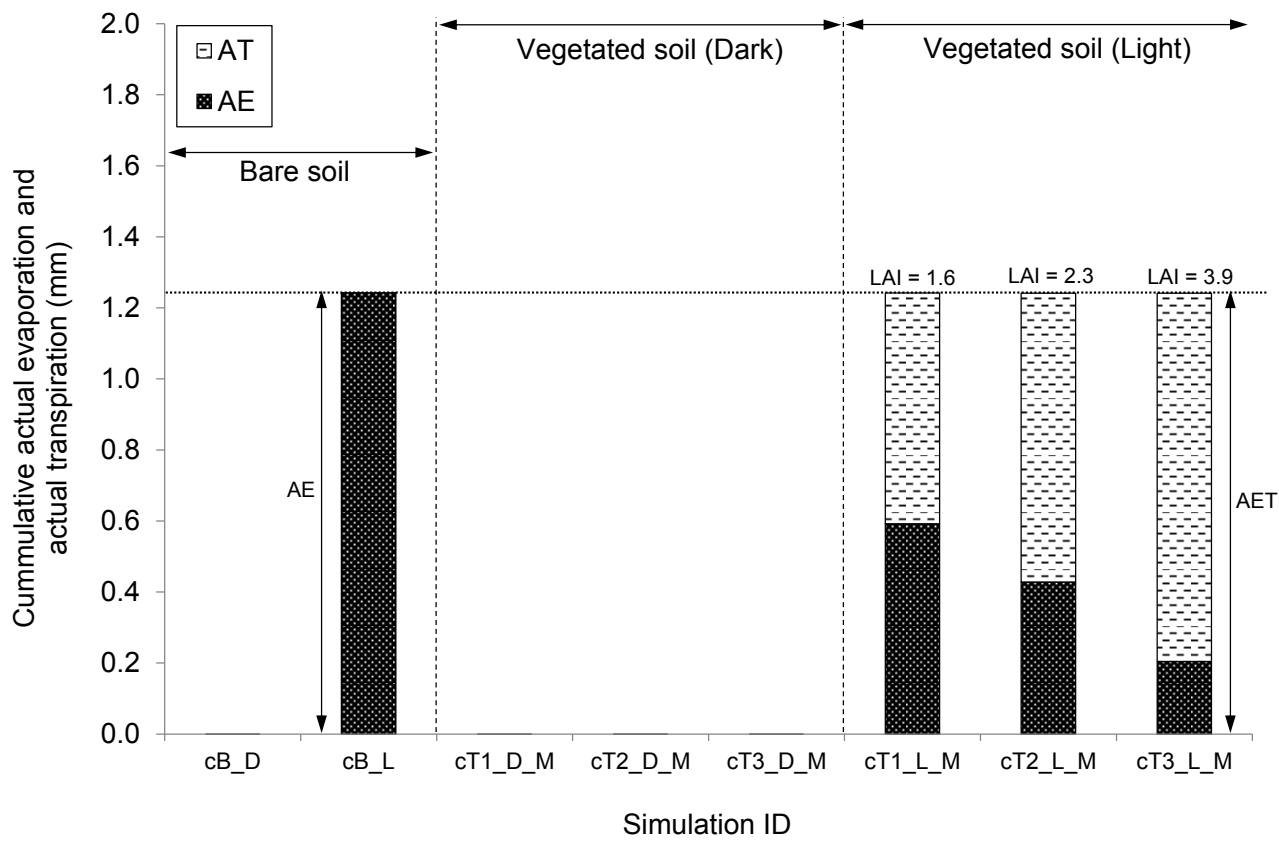
Fig. 12. Computed water balance in bare and vegetated soil after 12 hours of drying period